Earth and Planetary Science Letters xxx (2008) xxx–xxx

Contents lists available at ScienceDirect

Earth and Planetary Science Letters

journal homepage: www.elsevier.com/locate/epsl

# One hundred million years of mantle geochemical history suggest the retiring of mantle plumes is premature

Jasper G. Konter [a,*], Barry B. Hanan [b], Janne Blichert-Toft [c], Anthony A.P. Koppers [a,1], Terry Plank [d,2], Hubert Staudigel [a]

[a] SIO, University of California, San Diego, La Jolla, Ca, 92093, USA
[b] San Diego State University, San Diego, Ca, 92182-1020, USA
[c] Ecole Normale Supérieure de Lyon, CNRS UMR 5570, 69364 Lyon Cedex 7, France
[d] Boston University, Boston, Ma, 02215, USA

ARTICLE INFO

*Article history:*
Received 21 March 2008
Received in revised form 11 August 2008
Accepted 18 August 2008
Available online xxxx

Editor: R.W. Carlson

*Keywords:*
Pacific
seamount
Tokelau
Gilbert
hotspot
intraplate
plume
isotope
color coding

ABSTRACT

Linear chains of intraplate volcanoes and their geochemistry provide a record of mantle melting through geological time. The isotopic compositions of their lavas characterize their mantle sources, and their ages help backtrack these volcanoes to their original, eruptive source regions. Such data may shed light on a much-debated issue in Earth Sciences: the origin of intraplate volcanism and its underlying mantle and lithosphere dynamics. We show here that three major Western Pacific Seamount groups, ~50–100 million years in age, display distinct Sr, Nd, Hf, and Pb isotopic signatures that can be traced back in time, both geographically and geochemically, to three separate, recently-active intraplate volcanoes in the South Pacific Cook–Austral Islands. Their unique 100 million year history, which shows a persistent geochemical fingerprint, suggests formation from large volumes of laterally fixed, long-lived source regions. Such longevity is unlikely to be attained in the relatively dynamic upper mantle. Therefore, these sources are likely anchored deep in the mantle, isolated from homogenization by mantle convection, and imply a primary origin from deep mantle plumes rather than resulting from lithosphere extension.



## 1. Introduction

The "hotspot" hypothesis predicts that time-progressive linear chains of oceanic intraplate volcanoes (OIV) are formed on tectonic plates that pass over buoyantly rising plumes from fixed deep mantle sources (Morgan, 1971). However, an alternative mechanism has been proposed that explains OIV chains as shallow mantle melts rising to the surface along extensional lithospheric fractures (e.g. Foulger and Natland, 2003). Each of these models implies a profoundly different dynamic and chemical state, and hence evolution, of the Earth's mantle. We contribute to this debate with a comprehensive isotopic study of well-dated seamounts in the Western Pacific. We explore over 100 Ma of Sr–Nd–Hf–Pb isotope geochemical history of three prominent OIV groups in the Western Pacific: the Gilbert Ridge (64–78 Ma), the Tokelau chain (59–72 Ma), and the Western Pacific Seamount Province (WPSP, 80–140 Ma) (Fig. 1; Koppers et al., 2003; Koppers and Staudigel, 2005; Koppers et al., 2007). These three groups consist of chains of several kilometer tall volcanoes, often with rift zones and typically coral-capped. The chains are related to three geochemically distinct and active OIVs in the Cook–Austral region. Persistent eruption over 100 Ma from these sources requires substantial volumes that remained stable, which we consider unlikely to be located in the upper mantle. Combining our geochemical results with geophysical data and geodynamic models, we suggest that these volcanoes most likely formed from deep mantle plumes, while lithospheric cracks played a secondary role.

## 2. Background

The seamounts investigated in this work are located in the southwestern Pacific Ocean, between the Marianas Trench and the Samoan Islands, in the region between approximately 25°N and 10°S, and 150°E and 170°W (Fig. 1). Most of these seamounts are part of the Darwin Rise (Menard, 1964), a region heavily populated with seamounts. This area is very similar to the currently volcanically active south-central Pacific Ocean in terms of its shallow bathymetry, thin

* Corresponding author. Present address: University of Texas at El Paso, El Paso, Tx 79968, USA. Tel.: +1 915 747 5507; fax: +1 915 747 5073.
*E-mail addresses:* jgkonter@utep.edu, jkonter@ucsd.edu (J.G. Konter).
[1] Present address: Oregon State University, Corvallis, Or 97331, USA.
[2] Present address: Columbia University, Palisades, NY 10964, USA.

0012-821X/$ – see front matter © 2008 Elsevier B.V. All rights reserved.
doi:10.1016/j.epsl.2008.08.023

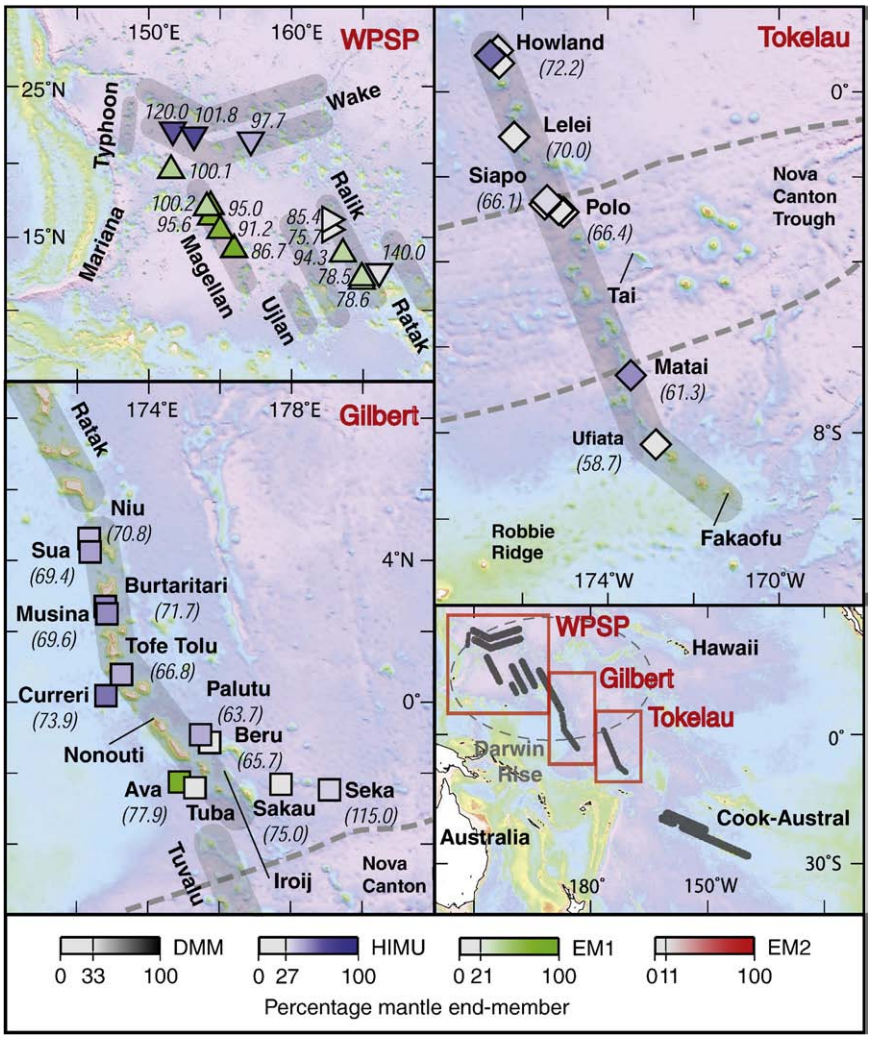


**Fig. 1.** Sample locations for the WPSP, Tokelau, and Gilbert lineaments, with an overview map on the lower right. Seamount chains are outlined with gray bands. Symbols are specific to seamount groups, and symbol colors indicate the dominant mantle end-member of a given sample (DMM, EMI, EMII, HIMU), whereby color saturation reflects the increasing percentage of that end-member (see scale at bottom; Supplementary data). Ages are from Ar–Ar dating of crystalline groundmass separates, and feldspar, amphibole and biotite separates.

elastic plate thickness (McNutt and Fischer, 1987; Smith et al., 1989; Wolfe and McNutt, 1991; Winterer et al., 1993; McNutt, 1998), and the large number of seamounts that span a geochemically wide range of isotopic compositions (Staudigel et al., 1991). These similarities, combined with plate motion models and paleolatitude estimates, have led some authors to suggest that the Darwin Rise is the Cretaceous analog to the currently-active South Pacific (McNutt and Fischer, 1987; Davis et al., 1989; Larson, 1991; Staudigel et al., 1991; Janney and Castillo, 1999; Koppers et al., 2003).

Volcanism in the south-central Pacific is characterized by the presence of closely spaced, typically short, discontinuous chains with extreme mantle source isotopic compositions (Staudigel et al., 1991). The observed geochemical signatures were recognized as part of the global DUPAL anomaly (Hart, 1984), although more than one extreme signature is present in the area (Staudigel et al., 1991). The origins of most of these signatures have been sought in recycling of crustal material into the mantle (Hofmann and White, 1982; White and Hofmann, 1982; Zindler and Hart, 1986). The wide variation in isotopic compositions reaches back into the Cretaceous western Pacific, and it has therefore been suggested that the sources of these volcanoes resulted from the subduction focusing of different types of recycled lithologies (Staudigel et al., 1991; Koppers et al., 2003).

Volcanic chains in the Southern and Western Pacific are often discontinuous and often not consistently age progressive, leading to a model of three contemporaneous hotspots for the Cook–Austral Islands (Chauvel et al., 1997; Dickinson, 1998; Koppers et al., 2003; Koppers et al., 2007). Alternatively, the existence of chains with a non-linear age distribution has led to other models such as mantle hotlines (Bonatti and Harrison, 1976), weak plumes (Sleep, 1984; Duncan et al., 1986; Woodhead, 1992; McNutt et al., 1997), or lithospheric cracking (Foulger and Natland, 2003). For example, the Pukapuka Ridge may have formed by tensional or uneven thermal cooling stress (Sandwell and Fialko, 2004; Gans et al., 2003). However, seismic tomography data of the Southwest Pacific suggest a thermo-chemical anomaly in the mantle that may represent an under-resolved group of plumes (e.g. Ekstrom and Dziewonski, 1998; Masters et al., 2000; Montagner, 2002; Romanowicz and Gung, 2002; Montelli et al., 2004; Schubert et al., 2004). Courtillot et al. (2003) accommodate the diversity of oceanic intraplate volcanoes by promoting three different types of hotspots: (1) Primary hotspots correspond to the original mantle plume concept of Morgan (1971) with single plumes rising from the deep mantle (e.g. the core–mantle boundary); (2) secondary hotspots reflect plumelets off the top of a superplume in the mantle transition zone, similar to weak plumes (Sleep, 1984; Duncan et al., 1986; Woodhead, 1992; McNutt et al., 1997);

Please cite this article as: Konter, J.G., et al., One hundred million years of mantle geochemical history suggest the retiring of mantle plumes is premature, Earth Planet. Sci. Lett. (2008), doi:10.1016/j.epsl.2008.08.023

(3) tertiary hotspots are interpreted to be the result of upwelling caused by lithospheric extension. The volcanic chains in the south-central and western Pacific have all been interpreted as secondary hotspots (Courtillot et al., 2003; Koppers et al., 2003).

Although long-lasting primary hotspots offer an important record of the geochemistry of the Earth's mantle, the secondary hotspots of the entire Southern Pacific province may provide a longer record. For example, primary hotspots such as the Hawaii–Emperor chain and the Louisville Ridge provide samples of mantle melting dating back to ~80 Ma (Regelous et al., 2003; Koppers et al. 2004), thus placing constraints on the large-scale geochemical history and structure of the regional mantle. However, volcanic chains in the Southern Pacific make up a much larger geochemical province that has been active for a substantially longer time, erupting lavas with a much wider geochemical range. Given that many chains are discontinuous and not obviously age progressive (e.g. Koppers et al., 2003), it remains uncertain which of the three hotspot types the seamount chains represent.

In this paper, we investigate the geochemical history of the southwest Pacific intraplate volcanic region to explore whether these chains can be used to provide a mantle source record even further back in time than Hawaii or Louisville. And equally importantly, we examine whether particular mantle source regions produce magmas of consistent geochemical fingerprints that may help resolve the origin of magmas in volcanic chains with inconsistent age progressions.

## 3. Methods

### 3.1. Analytical techniques and sample data

The 48 samples analyzed in this study include primarily alkali basalts and their differentiates (see Supplementary data for a brief description of the samples and additional analytical information). These include already-prepared samples from Koppers et al. (2003) for the WPSP for which Sr–Nd–Pb isotope data was available (but no Hf data) and samples from the AVON02 R/V Melville cruise in 1999 to the Gilbert Ridge and Tokelau Seamounts from which $^{40}Ar/^{39}Ar$ age data was available. All samples were leached prior to isotopic analysis to counter the effect of seafloor alteration. We measured Sr, Nd, Hf, and Pb isotope compositions for the entire sample suite (Table 1). Background data in diagrams were taken from the online Georoc and PetDB databases, Chauvel and Blichert-Toft, (2001), and Workman et al. (2004).

### 3.2. Isotopic analysis

Hf separation chemistry and mass spectrometric analysis followed the procedures of Blichert-Toft et al. (1997). All data were corrected for mass fractionation relative to $^{179}Hf/^{177}Hf = 0.7325$ using an exponential law. For comparison all data were normalized to JMC-475 $^{176}Hf/^{177}Hf = 0.282162$. The reproducibility within the measuring sessions was ±0.000003 ($2\sigma/\sqrt{n}$), while long-term external reproducibility was ± 0.000010 ($2\sigma$). Uncertainties reported on measured Hf isotope ratios are in-run $2\sigma/\sqrt{n}$.

Nd and Sr were separated and their isotopic compositions measured following Hanan et al. (2004, 2008). Sr isotope data were corrected for mass fractionation relative to $^{88}Sr/^{86}Sr = 0.1194$. SRM 987 averaged 0.710231 ± 9 ($2\sigma/\sqrt{n}$) over this period, but the data are reported relative to SRM 987 = 0.710243 to be consistent with the data of Koppers et al. (2003). Nd isotope data were corrected for mass fractionation by normalizing to $^{146}Nd/^{144}Nd = 0.7219$ using an exponential law. The La Jolla standard averaged 0.511844 ± 4 ($2\sigma/\sqrt{n}$) over this period, but all values have been normalized to La Jolla $^{143}Nd/^{144}Nd = 0.511851$ to be consistent with values of Koppers et al. (2003). Uncertainty on Nd isotope ratios are $2\sigma/\sqrt{n}$ of internal run statistics.

The Pb isotopic analyses were carried out by Tl doping (SRM 997 Tl and $^{205}Tl/^{203}Tl = 2.3889$; White et al., 2000; Hanan et al., 2004, 2008), using bracketing SRM 981 to correct for mass fractionation and machine bias (White et al., 2000). Bracketing SRM 981 values were adjusted to accepted values (Todt et al., 1996). The standard SRM 981 averaged $^{206}Pb/^{204}Pb = 16.934 \pm 4$, $^{207}Pb/^{204}Pb = 15.489 \pm 5$, and $^{208}Pb/^{204}Pb = 36.689 \pm 15$ ($2\sigma/\sqrt{n}$) over an extended period, whereas averages of individual sessions have $2\sigma/\sqrt{n}$ of $<0.001$ for $^{206}Pb/^{204}Pb$ and $^{207}Pb/^{204}Pb$, and $<0.002$ for $^{208}Pb/^{204}Pb$. The reported uncertainties of the data represent in-run precision including propagated standard reproducibility.

Duplicates were run for two samples and are the same within error for all the isotopes. The Hf duplicates were dissolved, processed, and measured in different labs (Ecole Normale Supérieure in Lyon and San Diego State University). BCR-1 also was analyzed and agrees within our reproducibility with literature data for trace elements (Table S1) and for isotopic ratios of leached material (Table 1; Weiss et al., 2006).

## 4. Analytical results

### 4.1. Removing the seawater contribution by leaching

The samples used in this study are splits of previously dated samples (Koppers and Staudigel, 2005; Koppers et al., 2007), and sample processing included leaching to minimize seafloor-weathering effects, following Koppers et al. (2003). A few samples from these seamounts have been analyzed previously, and confirm that alteration has significantly affected both major and trace element abundances, which therefore do not allow for meaningful petrologic modeling (Davis et al., 1989; Koppers et al., 2003). It has long been recognized that element exchange during acid-leaching also affects isotopic compositions of mobile elements, such as those in the Rb–Sr and U–Pb radiogenic isotope systems (Sr contribution from seawater and $^{206}Pb$ ingrowth from added U (e.g. Hauff et al., 2003)). However, sample leaching helps to obtain the original magmatic signatures by preferential dissolution of secondary phases (Shimizu and Hart, 1973; Koppers et al., 2003). Therefore, samples were leached (Koppers et al., 2003) prior to sample dissolution. In addition to leaching, we can also rely on relatively unaffected Hf and Nd isotope compositions (White and Patchett, 1984) to interpret magmatic source history.

For other isotope systems the effect of alteration can be gauged with a comparison between compositions of the leached whole rock and mineral separates of relatively unaltered phases from these samples. The Sr, Nd, Pb and Hf isotope compositions of mineral separates show good agreement with whole-rock data (Koppers et al., 2003; Table 1). Pyroxenes in particular show good agreement for Sr, Nd and Hf, but show some variations for Pb isotope compositions. Observed differences between pyroxenes and leached whole rocks are less than 0.0001, 0.00002, and 0.00002 for Sr, Nd and Hf respectively, therefore preserving the distinctions between most samples. However, Pb isotope ratios have been found to be heterogeneous even between fresh, zero-age whole rocks and their pyroxenes (e.g. Bryce and DePaolo, 2002). Therefore, small deviations in Pb isotope compositions could be the result of either magmatic processes or different degrees of alteration between rock and phenocrysts. Consequently, the agreement for all isotope systems between whole rocks and phenocrysts seems reasonable, showing minor disturbances from alteration. This suggests that our leached samples reflect a valid estimate of primary isotope compositions.

### 4.2. Age corrections and a worst-case scenario for radiogenic ingrowth

In order to compare the isotopic composition of mantle sources for our samples with each other and with recent volcanism in the Cook–Austral Islands, it is important to evaluate the effects of differential radiogenic ingrowth.

The effect from differential radiogenic ingrowth might be visible in Pb isotopic compositions, where the relatively shallow slopes of the Gilbert and Tokelau seamount chains could simply reflect ingrowth of

Please cite this article as: Konter, J.G., et al., One hundred million years of mantle geochemical history suggest the retiring of mantle plumes is premature, Earth Planet. Sci. Lett. (2008), doi:10.1016/j.epsl.2008.08.023

**Table 1**
Seamount compositional and meta-data

| Spl-name | Seamount (dredge) | Chain | Longitude | Latitude | Smt age | Error | $^{87}Sr/^{86}Sr$ | 2se | $^{143}Nd/^{144}Nd$ | 2se | $^{206}Pb/^{204}Pb$ | 2se | $^{207}Pb/^{204}Pb$ | 2se | $^{208}Pb/^{204}Pb$ | 2se | $^{176}Hf/^{177}Hf$ | 2se |
|---|---|---|---|---|---|---|---|---|---|---|---|---|---|---|---|---|---|---|
| Gilbert and Tokelau | | | | | | | | | | | | | | | | | | |
| NIU-2 | Niu (1) | Gilbert | 172.36 E | 4.63 N | 70.8 | 0.5 | 0.703326 | 2E−05 | 0.512813 | 8E−06 | 20.155 | 0.003 | 15.662 | 0.002 | 39.796 | 0.006 | 0.282907 | 4E−06 |
| SUA-1 | Sua (3) | Gilbert | 172.40 E | 4.25 N | 69.4 | 1.3 | 0.703153 | 3E−05 | 0.51258 | 1E−04 | 20.101 | 0.005 | 15.639 | 0.004 | 39.665 | 0.010 | 0.282942 | 6E−06 |
| BUR-2 | Burtaritari (4) | Gilbert | 172.82 E | 2.70 N | 71.7 | 0.4 | 0.703487 | 5E−05 | 0.512790 | 8E−06 | 20.582 | 0.002 | 15.722 | 0.002 | 40.231 | 0.005 | 0.282905 | 7E−06 |
| MUS-2 | Musina (5) | Gilbert | 172.88 E | 2.49 N | 69.6 | 0.6 | 0.703474 | 2E−06 | 0.512784 | 9E−06 | 20.546 | 0.002 | 15.722 | 0.002 | 40.305 | 0.005 | 0.282876 | 7E−06 |
| TOF-2 | Tofe Tolu (7) | Gilbert | 173.27 E | 0.78 N | 66.8 | 0.5 | 0.703237 | 3E−05 | 0.512850 | 7E−06 | 20.282 | 0.002 | 15.661 | 0.002 | 39.866 | 0.005 | 0.282907 | 6E−06 |
| CUR-1 | Curreri (9) | Gilbert | 172.84 E | 0.19 N | 73.9 | 0.8 | 0.703644 | 4E−05 | 0.512826 | 6E−06 | 19.316 | 0.002 | 15.637 | 0.002 | 39.280 | 0.004 | – | – |
| CUR-3 | Curreri (9) | Gilbert | 172.84 E | 0.19 N | 73.9 | 0.8 | 0.703557 | 1E−05 | 0.512809 | 9E−06 | 20.753 | 0.002 | 15.682 | 0.001 | 40.568 | 0.004 | – | – |
| NON-1 | Nonouti (12) | Gilbert | 174.11 E | 0.43 S | – | – | – | – | – | – | 20.043 | 0.004 | 15.622 | 0.003 | 40.930 | 0.011 | 0.282972 | 8E−06 |
| PAL-4 | Palutu (14) | Gilbert | 175.49 E | 0.92 S | 63.7 | 0.5 | 0.703130 | 2E−05 | 0.512861 | 1E−05 | 20.301 | 0.003 | 15.662 | 0.002 | 39.988 | 0.006 | 0.282953 | 7E−06 |
| BER-2 | Beru (16) | Gilbert | 175.74 E | 1.14 S | 65.7 | 0.7 | 0.703047 | 3E−06 | 0.512874 | 6E−06 | 19.862 | 0.002 | 15.647 | 0.002 | 39.631 | 0.005 | 0.282939 | 6E−06 |
| AVA-1 | Ava (18) | Gilbert | 174.90 E | 2.26 S | 77.9 | 0.5 | 0.706512 | 5E−06 | 0.512462 | 6E−06 | 17.728 | 0.001 | 15.547 | 0.001 | 38.492 | 0.004 | 0.282646 | 6E−06 |
| TUB-1 | Tuba (19) | Gilbert | 175.34 E | 2.41 S | – | – | 0.703185 | 2E−05 | 0.512998 | 8E−06 | 19.691 | 0.002 | 15.656 | 0.002 | 40.038 | 0.005 | 0.282943 | 7E−06 |
| IRO-1 | Iroij (22) | Gilbert | 176.10 E | 1.90 S | – | – | – | – | – | – | 20.579 | 0.004 | 15.681 | 0.003 | 40.446 | 0.008 | 0.282949 | 8E−06 |
| SAK-1 | Sakau (24) | Gilbert | 177.75 E | 2.31 S | 75.0 | 0.2 | 0.703533 | 3E−05 | 0.513057 | 8E−06 | 18.997 | 0.002 | 15.592 | 0.002 | 38.763 | 0.005 | 0.282885 | 1E−05 |
| SEK-1 | Seka (25) | Gilbert | 179.09 E | 2.48 S | 115.0 | 0.5 | 0.703000 | 2E−05 | 0.51310 | 2E−04 | 19.985 | 0.004 | 15.653 | 0.003 | 39.371 | 0.009 | 0.282922 | 6E−06 |
| *Duplicate* | | | | | | | | | | | 19.992 | 0.005 | 15.653 | 0.005 | 39.372 | 0.011 | 0.282919 | 5E−06 |
| HOW-3 | Howland (26) | Tokelau | 176.75 W | 0.84 N | 72.2 | 0.4 | 0.703086 | 8E−06 | 0.512965 | 8E−06 | 20.773 | 0.006 | 15.641 | 0.005 | 40.563 | 0.013 | 0.282956 | 6E−06 |
| HOW-7 | Howland (27) | Tokelau | 176.57 W | 0.97 N | 72.2 | 0.4 | 0.703021 | 1E−05 | 0.512976 | 7E−06 | 19.978 | 0.002 | 15.594 | 0.002 | 39.660 | 0.005 | 0.282940 | 7E−06 |
| HOW-9 | Howland (28) | Tokelau | 176.54 W | 0.67 N | 72.2 | 0.4 | 0.703083 | 2E−05 | 0.512909 | 8E−06 | 19.860 | 0.002 | 15.581 | 0.002 | 39.399 | 0.005 | 0.282939 | 7E−06 |
| LEL-2 | Lelei (34) | Tokelau | 176.19 W | 1.07 S | 70.0 | 0.5 | 0.702950 | 2E−05 | 0.512948 | 8E−06 | 19.790 | 0.002 | 15.581 | 0.002 | 39.555 | 0.005 | 0.282983 | 7E−06 |
| SIA-2 | Siapo (39) | Tokelau | 175.42 W | 2.60 S | 66.1 | 0.6 | 0.702931 | 3E−05 | 0.513010 | 7E−06 | 19.909 | 0.002 | 15.574 | 0.002 | 39.563 | 0.005 | 0.282992 | 6E−06 |
| SIA-6 | Siapo (40) | Tokelau | 175.43 W | 2.57 S | 66.1 | 0.6 | 0.702909 | 2E−05 | 0.513047 | 2E−05 | 19.952 | 0.004 | 15.592 | 0.003 | 39.622 | 0.007 | 0.283001 | 7E−06 |
| POL-2 | Polo (41) | Tokelau | 175.15 W | 2.78 S | 66.4 | 0.6 | 0.702912 | 1E−05 | 0.512988 | 9E−06 | 19.390 | 0.002 | 15.554 | 0.002 | 39.191 | 0.005 | 0.283055 | 5E−06 |
| POL-3 | Polo (41) | Tokelau | 175.15 W | 2.78 S | 66.4 | 0.6 | 0.702904 | 4E−05 | 0.512857 | 7E−06 | 19.418 | 0.002 | 15.557 | 0.002 | 39.255 | 0.005 | 0.283038 | 7E−06 |
| *Duplicate* | | | | | | | | | | | 19.418 | 0.005 | 15.558 | 0.006 | 39.255 | 0.019 | 0.283037 | 4E−06 |
| TAI-1 | Tai (42) | Tokelau | 173.41 W | 3.84 S | – | – | – | – | – | – | – | – | – | – | – | – | 0.283093 | 4E−06 |
| MAT-2 | Matai (48) | Tokelau | 173.47 W | 6.70 S | 61.3 | 0.6 | 0.706428 | 2E−05 | 0.512890 | 6E−06 | 20.310 | 0.002 | 15.611 | 0.002 | 40.533 | 0.005 | 0.282908 | 7E−06 |
| MAT-3 | Matai (49) | Tokelau | 173.47 W | 6.67 S | 61.3 | 0.6 | 0.703015 | 3E−06 | 0.512913 | 9E−06 | 20.546 | 0.004 | 15.606 | 0.003 | 40.676 | 0.007 | 0.282897 | 1E−05 |
| UFI-1 | Ufiata (57) | Tokelau | 172.88 W | 8.27 S | 58.7 | 0.3 | 0.703567 | 7E−07 | 0.512946 | 8E−06 | 19.758 | 0.002 | 15.547 | 0.002 | 39.528 | 0.005 | 0.282962 | 7E−06 |
| FAK-1 | Fakaofu (62) | Tokelau | 171.24 W | 9.21 S | – | – | – | – | – | – | 19.858 | 0.003 | 15.568 | 0.002 | 39.556 | 0.009 | 0.282993 | 7E−06 |
| CUR-21-cpx | Curreri (9) | Gilbert | 172.83 E | 0.19 N | 73.9 | 0.8 | – | – | 0.512839 | 4E−06 | – | – | – | – | – | – | 0.282944 | 6E−06 |
| CUR-22-cpx | Curreri (9) | Gilbert | 172.83 E | 0.19 N | 73.9 | 0.8 | – | – | 0.512844 | 5E−06 | – | – | – | – | – | – | 0.282945 | 5E−06 |
| ULU-cpx | Ulu (30) | Tokelau | 176.24 W | 0.40 S | – | – | – | – | 0.512848 | 5E−06 | – | – | – | – | – | – | 0.282961 | 2.5E−05 |
| BCR-1 | | | | | | | – | – | – | – | 18.800 | 0.002 | 15.619 | 0.002 | 38.803 | 0.006 | 0.282872 | 4E−06 |

| Spl-Name | Seamount | Chain | Longitude | Latitude | Group | Smt age | Error | $^{87}Sr/^{86}Sr$ | 2se | $^{143}Nd/^{144}Nd$ | 2se | $^{206}Pb/^{204}Pb$ | 2se | $^{207}Pb/^{204}Pb$ | 2se | $^{208}Pb/^{204}Pb$ | 2se | $^{176}Hf/^{177}Hf$ | 2se |
|---|---|---|---|---|---|---|---|---|---|---|---|---|---|---|---|---|---|---|---|
| WPSP | | | | | | | | | | | | | | | | | | | |
| HEM-1-U | Hemler | Solitary | 151.57 W | 19.55 N | Pit | 99.5 | 1.2 | *0.704761* | *<14e−6* | *0.512758* | *<15e−6* | *19.292* | – | *15.643* | – | *40.586* | – | 0.282843 | 6E−06 |
| HEM-2 | Hemler | Solitary | 151.57 W | 19.55 N | Pit | 100.7 | 1.2 | *0.704710* | *<14e−6* | *0.512736* | *<15e−6* | 18.991 | 0.004 | 15.673 | 0.003 | 39.380 | 0.010 | – | – |
| IOA-4 | Ioah | Magellan | 155.98 W | 14.18 N | Pit | 86.7 | 0.6 | *0.705002* | *<14e−6* | *0.512391* | *<15e−6* | 18.128 | 0.002 | 15.640 | 0.002 | 38.416 | 0.005 | 0.282625 | 7E−06 |
| LIK-1 | Likelep | Ujlan | 160.37 W | 10.60 N | Pit | 82.8 | 0.4 | *0.705313* | *<14e−6* | – | – | 18.509 | 0.002 | 15.622 | 0.001 | 38.673 | 0.003 | 0.282793 | 6E−06 |
| LIK-2 | Likelep | Ujlan | 160.37 W | 10.60 N | Pit | 82.4 | 0.4 | – | – | – | – | 18.547 | 0.002 | 15.628 | 0.002 | 38.827 | 0.005 | 0.282766 | 6E−06 |
| LIM-4 | Limalok | Ratak | 172.35 W | 5.55 N | Pit | 68.0 | 0.6 | – | – | – | – | 18.818 | 0.002 | 15.650 | 0.002 | 38.373 | 0.004 | 0.282867 | 8.0E−05 |
| LOB-1 | Lobbadede | Ralik | 163.62 W | 13.87 N | Pit | 94.3 | 0.5 | *0.703877* | *<14e−6* | *0.512678* | *<15e−6* | 19.032 | 0.003 | 15.675 | 0.003 | 38.726 | 0.007 | 0.282806 | 4E−06 |
| OMA-1-L | Vlinder | Magellan | 154.35 W | 16.40 N | Pit | 95.6 | 0.7 | *0.704606* | *<14e−6* | *0.512541* | *<15e−6* | 18.386 | 0.003 | 15.623 | 0.002 | 38.636 | 0.006 | 0.282757 | 7E−06 |
| PAK-3 | Pako | Magellan | 155.02 W | 15.50 N | Pit | 91.2 | 0.4 | *0.705192* | *<14e−6* | *0.512562* | *<15e−6* | 18.626 | 0.002 | 15.633 | 0.002 | 38.812 | 0.004 | 0.282736 | 8E−06 |
| VLI-1-L | Vlinder | Magellan | 154.33 W | 17.12 N | Pit | 95.0 | 0.7 | *0.704652* | *<14e−6* | *0.512517* | *<15e−6* | 18.121 | 0.002 | 15.600 | 0.002 | 38.256 | 0.004 | 0.282761 | 7E−06 |
| VLI-5-L | Vlinder | Magellan | 154.07 W | 17.03 N | Pit | 100.2 | 0.4 | *0.704558* | *<14e−6* | *0.512738* | *<15e−6* | 19.094 | 0.008 | 15.669 | 0.007 | 39.331 | 0.018 | 0.282830 | 5E−06 |
| WOD-2-L | Wodajebato | Ralik | 164.93 W | 12.00 N | Pit | 78.6 | 1.0 | *0.704722* | *<14e−6* | *0.512766* | *<15e−6* | 19.478 | 0.007 | 15.651 | 0.006 | 39.378 | 0.014 | – | – |
| WOD-3 | Wodajebato | Ralik | 164.93 W | 12.25 N | Pit | 78.5 | 1.7 | *0.704755* | *<14e−6* | *0.512767* | *<15e−6* | 19.429 | 0.002 | 15.634 | 0.002 | 39.261 | 0.005 | 0.282952 | 5E−06 |
| ALC-1 | Alcatraz | N Wake | 149.95 W | 24.10 N | C | 113.0 | 0.9 | – | – | – | – | 19.018 | 0.004 | 15.594 | 0.003 | 38.786 | 0.007 | 0.283011 | 6E−06 |
| MIS-2 | Missy | S Wake | 154.93 W | 20.95 N | C | 96.7 | 0.9 | – | – | – | – | 19.040 | 0.004 | 15.625 | 0.003 | 38.914 | 0.008 | 0.283105 | 4E−06 |
| MIT-4 | MIT | Solitary | 151.88 W | 27.32 N | C | 123.9 | 1.4 | – | – | – | – | 19.212 | 0.002 | 15.590 | 0.001 | 38.518 | 0.004 | 0.282974 | 8E−06 |
| NWO-1 | N Wod-En | Ralik | 162.93 W | 15.97 N | C | 85.4 | 1.0 | *0.703645* | *<14e−6* | *0.512848* | *<15e−6* | 19.758 | 0.002 | 15.624 | 0.002 | 39.379 | 0.005 | – | – |
| SET-4 | Seth | Typhoon | 148.68 W | 23.82 N | C | 139.3 | 0.7 | – | – | – | – | 19.491 | 0.002 | 15.567 | 0.002 | 39.124 | 0.003 | 0.283013 | 6E−06 |
| SWO-1 | S Wod-En | Ralik | 162.93 W | 15.28 N | C | 75.7 | 0.9 | *0.703327* | *<14e−6* | *0.512856* | <15e−6 | *19.684* | – | *15.619* | – | *39.990* | – | – | – |
| GLD-5-L | Golden Dragon | S Wake | 153.15 W | 21.37 N | Tub | 101.8 | 0.5 | *0.703388* | *<14e−6* | *0.512866* | <15e−6 | 21.095 | 0.004 | 15.759 | 0.003 | 41.638 | 0.009 | 0.282925 | 6E−06 |
| HIM-2 | Himu | S Wake | 150.70 W | 20.70 N | Tub | 119.5 | 1.2 | – | – | – | – | 20.709 | 0.012 | 15.715 | 0.010 | 40.277 | 0.025 | 0.282924 | 6E−06 |
| HIM-3 | Himu | S Wake | 151.70 W | 21.70 N | Tub | 120.0 | 1.6 | *0.702776* | *<14e−6* | *0.512899* | *<15e−6* | *20.893* | – | *15.723* | – | *40.405* | – | 0.282901 | 6E−06 |
| LOO-2 | Look | Solitary | 166.15 W | 12.15 N | Tub | 140.0 | 1.6 | *0.702904* | *<14e−6* | *0.512839* | *<15e−6* | 19.848 | 0.003 | 15.698 | 0.002 | 39.474 | 0.005 | 0.282809 | 7E−06 |
| MAL-2-L | Maloney | S Wake | 157.15 W | 21.05 N | Tub | 97.7 | 0.6 | *0.703245* | *<14e−6* | *0.512843* | *<15e−6* | *20.595* | – | *15.689* | – | *39.906* | – | – | – |
| VLI-5-cpx | Vlinder | Magellan | 154.07 W | 17.03 N | Pit | 100.2 | 0.4 | – | – | 0.512741 | 6E−06 | – | – | – | – | – | – | 0.282840 | 9E−06 |
| NWO-1-cpx | N Wod-En | Ralik | 162.93 W | 15.97 N | C | 85.4 | 1.0 | – | – | 0.512852 | 6E−06 | – | – | – | – | – | – | 0.282978 | 3E−06 |
| GLD-5-cpx | Golden Dragon | S Wake | 153.15 W | 21.37 N | Tub | 101.8 | 0.5 | – | – | 0.512876 | 5E−06 | – | – | – | – | – | – | 0.282911 | 4.4E−05 |
| MAL-2-cpx | Maloney | S Wake | 157.15 W | 21.05 N | Tub | 97.7 | 0.6 | – | – | 0.512855 | 6E−06 | – | – | – | – | – | – | 0.282917 | 5.0E−05 |

Key: Smt age = Seamount age; cpx = clinopyroxene.
Isotopic ratios in italics and ages from Koppers et al. (2003, 2007); Koppers and Staudigel (2005).



Please cite this article as: Konter, J.G., et al., One hundred million years of mantle geochemical history suggest the retiring of mantle plumes is premature, Earth Planet. Sci. Lett. (2008), doi:10.1016/j.epsl.2008.08.023

samples with varying U/Pb (Fig. 2). This can be evaluated through age-corrected isotope compositions. Unfortunately we cannot accurately determine all of the required data in our altered samples. While we consider the ages and the isotopic ratios as quite reliable, whole-rock parent/daughter ratios are not, in particular the Rb/Sr and the U/Pb ratios. Although data from fresh primary minerals may provide a proxy for lava parent/daughter ratios, significant uncertainty remains from assumptions about unconstrained petrogenetic parameters (e.g. partitioning during melting and crystallization). Instead, we feel that a worst-case scenario approach can provide a better constrained upper bound on the possible differences by forward calculating the isotopic compositions of a highly parent/daughter-depleted DMM-type source and a highly-enriched Cook–Austral Islands lava.

For Pb isotopes we assess this worst-case scenario with an extremely high value for $^{238}U/^{204}Pb$ ($\mu$=42.85 estimated from published U/Pb; Willbold and Stracke, 2006) for the lava, and a low value for the source ($\mu$=12.20, DMM composition; Workman and Hart, 2005). As a consequence of the short $^{235}U$ half-life, low $^{235}U/^{204}Pb$ ratios lead to only minor ingrowth of $^{207}Pb$, while the major effect is visible in $^{206}Pb/^{204}Pb$ with a 0.4 increase for the enriched lava, compared to 0.1 for the source over 60 Ma (corresponding to the age difference between Gilbert/Tokelau samples with either WPSP or present volcanism).

The difference of 0.3 in the $^{206}Pb/^{204}Pb$ ratios is smaller than the range within individual chains, and far smaller than the total range for all samples. Therefore, large-scale isotopic trends remain robust, even though the individual slopes in a $^{206}Pb/^{204}Pb$–$^{207}Pb/^{204}Pb$ diagram may be disturbed. In fact the upper bound-difference of 0.3 in $^{206}Pb/^{204}Pb$ changes the slope enough to increase the secondary isotope age from 800 Ma to almost 2 Ga. Therefore, correction for this effect may bring the slopes closer to the mantle array.

We expect smaller effects in isotopic systems with longer half-lives, such as Nd and Sr, compared to Pb. Using parent/daughter ratios based on the same sources (Workman and Hart, 2005; Willbold and Stracke, 2006) we find worst-case scenario differences between enriched lavas and depleted sources of 0.00004 and 0.0002 in $^{143}Nd/^{144}Nd$ and $^{87}Sr/^{86}Sr$, respectively. Although these differences are larger than the analytical uncertainty, they are very small in comparison with the range in our data. Therefore, the main effect is likely to be observed in the Pb isotope ratios. These calculations show that the measured isotope ratios are a reasonable representation of the mantle source signature of the lavas and can be used to interpret the large-scale variations in our data set.

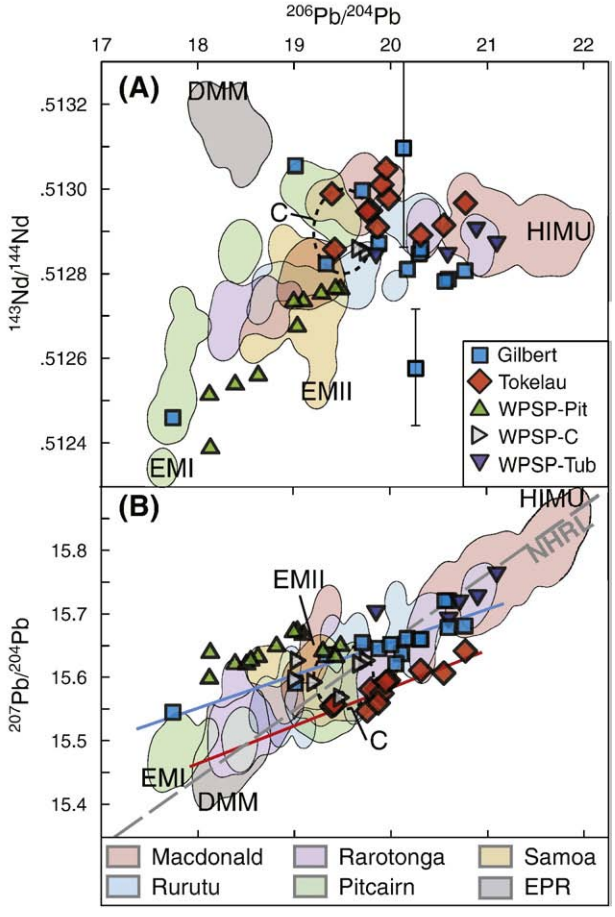


**Fig. 2.** Nd–Pb (A) and Pb–Pb (B) isotope compositions compared to representative fields for oceanic basalts (taking analytical uncertainty into account). Mantle end-members are approximated by a central ellipse ("C") and data from the East Pacific Rise (EPR; DMM), Pitcairn (EMI), Samoa (EMII), and hotspots of the Cook–Austral Islands (HIMU): Macdonald (includes e.g. Tubuai and Mangaia), young Rurutu, and Rarotonga (Georoc and PetDB). (A) Isotopic compositions of Gilbert seamounts are similar to young Rurutu, Tokelau seamounts correspond well to Macdonald, and Magellan, Ralik, Hemler Seamount and Ujlan (WPSP-Pit) are similar to Rarotonga. Northern and southern Wake, Typhoon, MIT, and Wod-En (WPSP-C) have intermediate isotopic compositions, and Southern Wake and Look Seamount (WPSP-Tub) are similar to the Macdonald and Rurutu hotspots. The Pb–Pb trend (B) for all oceanic basalts is steeper than the Gilbert and Tokelau trends. Error bars (2$\sigma$) are shown when larger than the symbol size.

### 4.3. Radiogenic isotopes

Most of our samples have isotopic compositions between C and HIMU or C and EMI, similar to the volcanic chains of the Tubuai and Pitcairn Islands, respectively (Fig. 2; end-member compositions see Supplementary Table S4). However, small (but distinct) differences exist between the different seamount groups, particularly between the WPSP group and both the Gilbert and Tokelau groups. The Gilbert Ridge ranges from 0.512462–0.513096 in $^{143}Nd/^{144}Nd$, 0.703000–0.706512 in $^{86}Sr/^{86}Sr$, 17.728–20.753 in $^{206}Pb/^{204}Pb$, and 0.282646–0.282972 in $^{176}Hf/^{177}Hf$. This compositional range is very similar to the (young) Rurutu hotspot (Fig. 2). Ava seamount is an outlier with the lowest Nd, lowest Hf, and highest Sr, also located off the seamount chain with a relatively old age (Koppers et al., 2007). The Tokelau chain has a narrower compositional range, similar to the Macdonald hotspot (Fig. 2) ($^{143}Nd/^{144}Nd$=0.512857–0.513047; $^{86}Sr/^{86}Sr$=0.702904–0.706428; $^{206}Pb/^{204}Pb$=19.390–20.773; $^{176}Hf/^{177}Hf$=0.282897–0.283093). However, the $^{207}Pb/^{204}Pb$ ratios of the Tokelau seamounts straddle the edge of the field for Macdonald hotspot. Fig. 2 and Supplementary Figure S4 also show that the samples have on average somewhat higher $^{143}Nd/^{144}Nd$ and $^{176}Hf/^{177}Hf$, and lower $^{207}Pb/^{204}Pb$ than the Gilbert array, and form a parallel array, while both arrays have a shallower slope than the mantle array and the Northern Hemisphere Reference Line (NHRL; Hart, 1984). However, the observed slopes could simply be an artifact of radiogenic ingrowth, and an age correction could place the deviating Tokelau samples inside the Macdonald field.

For the WPSP group our Pb and Hf isotope data supplement the isotope data of Koppers et al. (2003). The WPSP can be subdivided into three compositional groups (see Table 1, Fig. 2), with samples similar to Pitcairn volcanoes (WPSP-Pit) ranging from 0.512391–0.512767 in $^{143}Nd/^{144}Nd$, 0.703877–0.705313 in $^{86}Sr/^{86}Sr$, 18.121–19.478 in $^{206}Pb/^{204}Pb$, and 0.282625–0.282952 in $^{176}Hf/^{177}Hf$. Samples from WPSP-C scatter around a C-type composition ($^{143}Nd/^{144}Nd$=0.512848–0.512856; $^{86}Sr/^{86}Sr$=0.703327–0.703645; $^{206}Pb/^{204}Pb$=19.018–19.758; $^{176}Hf/^{177}Hf$=0.282974–0.283105). Finally, WPSP-Tub samples are similar in composition to the Tubuai Islands ($^{143}Nd/^{144}Nd$=0.512839–0.512899; $^{86}Sr/^{86}Sr$=0.702776–0.703388; $^{206}Pb/^{204}Pb$=19.848–21.095; $^{176}Hf/^{177}Hf$=0.282809–0.282925).

In summary, the entire data set spans a substantial part of the total compositional variation in OIVs, yet each of the individual OIV groups or seamount trails has a unique isotopic signature. Interestingly, the overall compositional variation is observed in the Cook–Austral Islands as well, an area representing the seamounts' source region (Fig. 2).

Please cite this article as: Konter, J.G., et al., One hundred million years of mantle geochemical history suggest the retiring of mantle plumes is premature, Earth Planet. Sci. Lett. (2008), doi:10.1016/j.epsl.2008.08.023

## 5. Discussion

The study of the long-term geochemical evolution of specific mantle source regions requires a reliable method to relate dated and analyzed seamount samples to their original eruptive locations. Absolute Plate Motion models (APMs) offer such a method. If combined with isotopic compositions, APMs can help assess the geochemical composition of mantle sources in both space and time through representation in various map views. In the following sections, we color code the APM-reconstructed eruptive locations by their geochemical composition (Compositional Color Coding; see online Supplementary data) to investigate the longevity of mantle source domains back into Cretaceous times. In addition, we investigate the age and origin of these sources to constrain mantle structure.

### 5.1. Absolute Plate Motion models

In order to constrain the location of the mantle source regions of a seamount on a moving plate, we have to reliably reconstruct their eruptive location with respect to its mantle reference frame. Our best estimate of this type of Absolute Plate Motion derives from APMs that are based on the assumption that oceanic volcanic chains represent the surface expression of plates moving over fixed or relatively slow moving mantle plumes. APMs are typically constructed using the trend and location of several volcanic chains on a plate and in indirect ways the age of volcanoes within them (Wessel and Kroenke, 1997; Koppers et al., 2001; Kroenke et al., 2004; Wessel et al., 2006). However, these models are based on decreasing amounts of data when going back in time, resulting in an increasing reconstruction error for older plate motion stages. APM stages younger than 5 Ma are accurately known as they have been validated by independent measurements of current plate motion (GPS, Satellite Laser Ranging; e.g. Altamimi et al., 2002). Despite this independent evidence for plate motion, it has been pointed out that discrepancies nevertheless occur, even between young chains. Specifically, volcano ages and paleomagnetic data have recently suggested that the mantle plume sources for the Emperor and Louisville chains actually may have moved as a result of variations in mantle convection patterns (Steinberger, 2000; Tarduno et al., 2003; Koppers et al., 2004; Steinberger et al., 2004). However, such plume motion only becomes significant for reconstructions for the older parts of volcanic chains, due to the relative magnitude of plate versus plume motion (O'Neill et al., 2005). Irrespective of the possible motion, APMs appear to provide a number of first-order predictions, such as a general direction of plate motion over the last ~50 Ma and a cumulative direction from a combined plate and plume motion for periods prior to that.

For an interpretation using APMs it is important to remember that the oldest seamount chains have larger reconstruction errors. Since chains older than the Hawaiian–Emperor chain (>80 Ma) were part of the construction of some APMs, there are no independent constraints on the backtracked locations. Here, we consider APMs older than 80 Ma as less reliable, because they lack independent support from seamounts other than those studied here (Koppers et al., 2003). Other reconstruction errors arise from geological complications: (a) OIV volcanoes can be active for 10 Ma or longer (e.g. Hoernle and Schmincke, 1993) allowing younger lavas to cover the oldest volcanism, (b) samples from volcanic rift zones and lava flows that traveled long distances are offset from the source location where magma ascended into the crust, and (c) volcanic centers themselves may be offset from their sources by lateral magma transport due to lithospheric structure (Koppers et al., 2003; Koppers and Staudigel, 2005). These factors result in cumulative uncertainties in eruptive locations of up to hundreds of kilometers, predicting elongated clusters of eruptive locations around a single source.

The uncertainties may be quantified using the misfit of reconstructed eruptive locations based on ages for volcanoes used in creating APMs. The misfit calculated by Wessel et al. (2006) for their APM defines an elliptical shape with a long axis of ~5.5°. However, their misfit only includes reconstructed volcanoes dated back to just under 80 Ma. Given the increasing APM uncertainty with age, the misfit will likely be larger when older seamounts are included.

With these uncertainties in mind, we reconstructed the eruptive locations of our seamounts with several APMs including several Pacific volcanic chain derived models, a model that includes plume motion and one using the Indo-Atlantic hotspot reference frame. Due to the increased uncertainties related to the oldest stages of APMs, we also separated seamounts older than 80 Ma from younger seamounts (Figs. 3, 4). In Fig. 3 we show the backtracking of these seamounts with one of the most recent APMs (W06; Wessel et al., 2006). The newest model by Wessel and Kroenke (2008) partly relies on the Gilbert and Tokelau chains in its construction and is therefore less suitable for our reconstructions. Reconstructions with W06 in Fig. 3 show clusters of reconstructed eruptive locations for the studied seamounts. The sizes of the clusters have 95% confidence ellipses (after rejecting outliers outside $3\sigma$) that are very similar in size to the predicted uncertainty of W06, particularly for the Gilbert and Tokelau seamounts. The ellipse calculated for the older WPSP seamounts is larger and similar to that of Wessel and Kroenke (2008), which is expected due to the larger errors associated with APMs stretching back into time beyond 80 Ma. The existence of these clusters then leads to the question whether each cluster is simply related to a single source, which can be evaluated using the geochemical compositions of the seamounts.

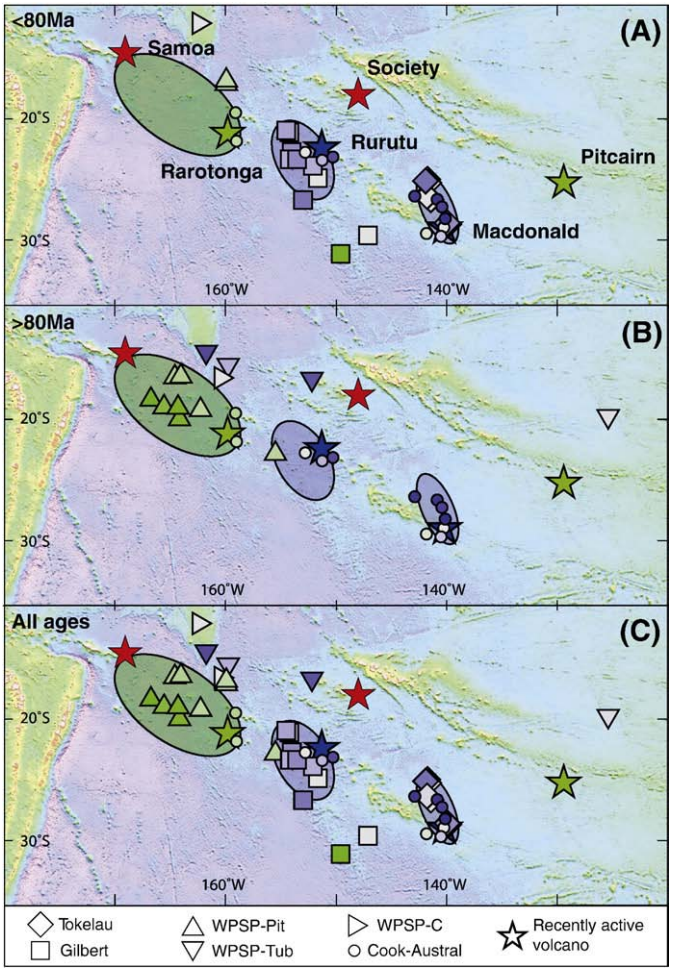


**Fig. 3.** Backtracked (Wessel et al., 2006) sample locations color-coded by composition (see Fig. 1 and Supplementary data) for (A) the Gilbert and Tokelau seamounts, (B) the WPSP, and (C) the combined data sets. Stars indicate the location and geochemical end-member type of recently-active volcanoes. The backtracked seamount data define three regional clusters with geochemical signatures that are consistent with three distinct 0–20 Ma hotspots proposed for the Cook–Austral Island chain (small circles), at Macdonald, Rurutu, and Rarotonga (Chauvel et al., 1997).

Please cite this article as: Konter, J.G., et al., One hundred million years of mantle geochemical history suggest the retiring of mantle plumes is premature, Earth Planet. Sci. Lett. (2008), doi:10.1016/j.epsl.2008.08.023

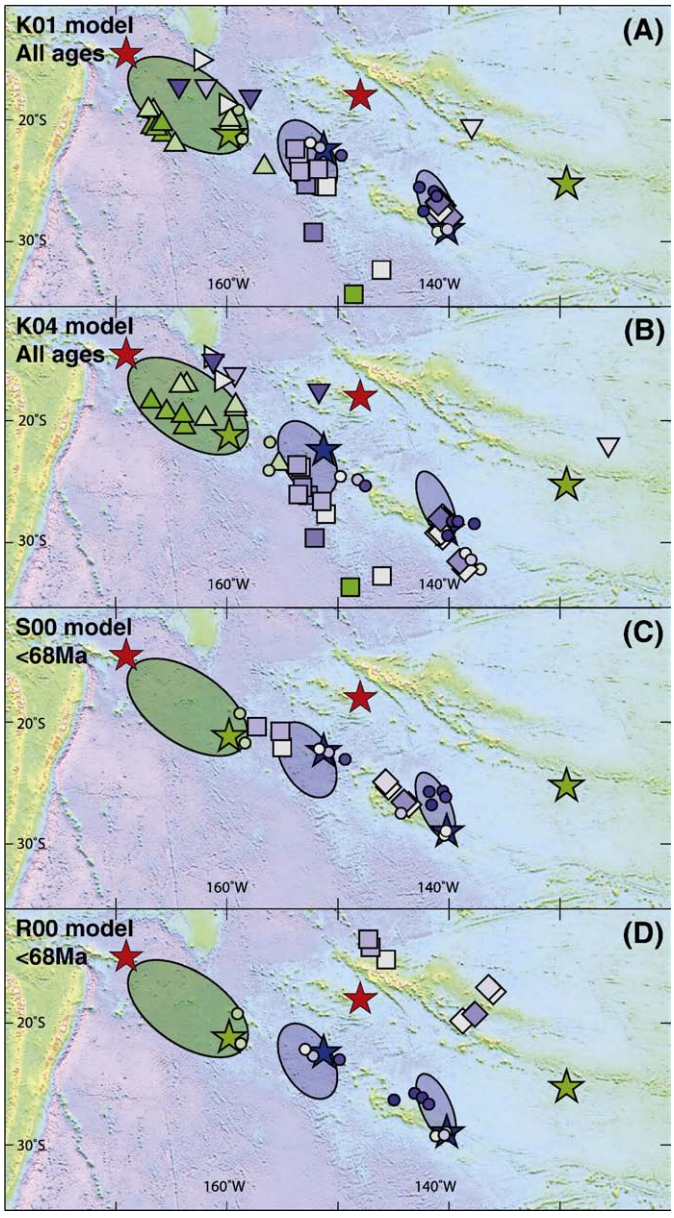


**Fig. 4.** Backtracked eruptive locations (color-coded by composition) using four published plate motion models, including (A) plate motion history back to 140 Ma based on chain geometry and seamount ages (Koppers et al., 2001), (B) motion back to 140 Ma based on chain geometry also fitting the last 3 Ma in Hawaii (Kroenke et al., 2004), (C) motion back to 68 Ma based on a moving plume due to mantle flow (Steinberger, 2000), (D) motion back to 68 Ma based on motion with respect to Indo-Atlantic hotspots (Raymond et al., 2000). Compared to the latest APM (Wessel et al., 2006), the clusters formed in (A) are most similar, as can be seen from the agreement between the backtracked locations and the outlined ellipses (clusters) found with Wessel et al. (2006). Significant overlap can still be seen in (B) and (C), but the locations in (D) do not overlap at all.

In order to relate compositional characteristics of our seamount samples to their original, backtracked locations, we color-coded sample location symbols by mantle geochemical components (see also Fig. 1). The color codes indicate a given samples' dominating mantle end-member: HIMU, EMI, EMII, or DMM. The coloring in the scale bars is based on a statistical analysis that is presented in detail in the Supplementary data (Compositional Color Coding). Scale bars originate in the center of the Sr–Nd–Pb isotope array (near C and FOZO) and start out with a gray color. Saturated colors indicate the pure end-members in the ocean island array (Zindler and Hart, 1986; Hart et al., 1992, Hanan and Graham, 1996). The intermediate (mixed) colors show a samples' isotopic composition between the center and the dominating end-member. The gray areas in the scale bars are limited with a tick and a percentage, giving the data range for which a particular sample cannot be realistically separated from the central cluster of all ocean island basalts taken from the PetDB and GeoRoc databases.

Our results show that the backtracked seamounts cluster at three distinct locations, whereby reconstruction of seamounts younger than 80 Ma (Fig. 3A) show overlap with the currently-active Macdonald Seamount and (young) Rurutu hotspots in the Cook–Austral Islands (Chauvel et al., 1997). The third cluster is formed by seamounts mainly from the Magellan (>80 Ma; Fig. 3B) and Ralik (<80 Ma) seamounts, which overlap with the Rarotonga hotspot in the Cook–Austral Islands. However, in general for the seamounts older than 80 Ma, we see more variance, which is to be expected given the greater uncertainty in older plate motion stages. The largest discrepancies are caused by the oldest WPSP seamounts (100–140 Ma) that appear to reconstruct further north with larger uncertainty. Combining both age groups, more than 70% of the data fall within these clusters (Fig. 3C) using the W06 model. In Fig. 4 we show the results of the same reconstruction using four older APM models, which show the same three clusters, overlapping 50–100% with the geographical location in the most recent W06 model.

Despite the similarity in location and diameter of eruptive location clusters (5°–6°), there are some differences:

(1) The oldest Pacific, fixed plume model considered here (K01; Koppers et al., 2001) corresponds most closely to the outlined clusters of the W06 model, which is based on a geometric technique of finding stages of plate motion (Fig. 4A). However, the K01 model defines fewer stages consequently averaging small deviations in plate motion in the W06 model, which results in small deviations in reconstructed locations.

(2) Results from the other fixed plume model (K04; Kroenke et al., 2004) show, in general, the same relative locations for individual eruptive locations, but are offset, since the W06 model mainly differs in the way the last 3 Ma in the Hawaiian Islands are fit. This trend bends significantly southward, and thus produces a north–south difference between K04 and W06 (Fig. 4B).

(3) The model incorporating plume motion due to mantle flow (S00; Steinberger, 2000) backtracks to form two clusters of locations slightly further to the west, but still overlaps with the outlined W06 clusters. Since the S00 model is only defined from the present to 68 Ma, only seamounts younger than 68 Ma can be backtracked (Fig. 4C). Because plume motion will only become apparent as deviation from model prediction for the oldest volcanic chains (O'Neill et al., 2005), this comparatively short age range limits any possible observations of plume motion.

(4) Finally, the model for Pacific hotspot motion in the Indo-Atlantic framework (R00; Raymond et al., 2000) has to be rotated into the Pacific Ocean through a plate circuit of relative plate motions, introducing large uncertainty to the predicted plate motion (Steinberger et al., 2004). In fact, this model does not produce a bend in volcanic chains at ~45 Ma and is only defined for 0–68 Ma, resulting in two clusters of lesser-constrained locations (Gilbert and Tokelau) located further north (Fig. 4D).

Based on the above reconstructions we can conclude that irrespective of the APM used, clusters of backtracked locations are found to correspond to active hotspot volcanism within the Cook–Austral Islands (Chauvel et al., 1997), except for the R00 model that has a much larger associated error. In fact, by augmenting the number and density of backtracked island locations in the Cook–Austral Islands (less than ~20 Ma), our reconstructions strengthen the suggestion that these islands are the result of active volcanism in three separate locations (Chauvel et al., 1997). Furthermore, the S00 model, including plume motion, yields similar results to fixed plume models, suggesting that overall plume motion may be present, but secondary to plate

Please cite this article as: Konter, J.G., et al., One hundred million years of mantle geochemical history suggest the retiring of mantle plumes is premature, Earth Planet. Sci. Lett. (2008), doi:10.1016/j.epsl.2008.08.023

motion. More importantly, these backtracking reconstructions provide a temporal record for three intraplate volcanic areas back to the Cretaceous, and in combination with the geochemical composition of the volcanoes, they provide a substantial, long-lived record of mantle source evolution.

### 5.2. Mantle source compositions over 100 Ma

The compositional range of the "mantle array" is largely constructed with isotope data from relatively young OIVs, while our data come from volcanoes that are substantially older. Since partial melting will fractionate parent–daughter ratios, radiogenic decay will lead to more radiogenic Sr and Pb isotope ratios, and less radiogenic Nd and Hf ratios in the melt. We have shown in Section 4.2 that the measured isotope ratios provide reliable constraints on the mantle source signatures on a large scale.

The two major isotopic ranges found in the seamount lavas, between HIMU and C and between EMI and C, appear as three clusters of reconstructed eruptive locations with distinct compositional ranges. HIMU-C seamounts in the Wake, Tokelau, and Gilbert chains backtrack to areas either around Macdonald seamount or young Rurutu, whereas the EMI-C seamounts from mainly the Magellan and Ralik chains backtrack to near Rarotonga (Fig. 3). Given the respective isotopic compositions of the Cook–Austral hotspots (e.g. Chauvel et al., 1997), there is a remarkable compositional match between each cluster and the hotspot it is located around.

The close proximity of three persistent and isotopically distinct mantle regions leads us to speculate that they may have formed in a common subduction zone setting. Subduction-related mantle source components could include recycled oceanic crust, sediments, continental lithospheric materials or metasomatically enriched mantle wedge material (Hofmann and White, 1982; White and Hofmann, 1982; Zindler and Hart, 1986; Eiler et al., 1997; Jackson et al. 2007). Sr–Nd–Hf–Pb–Os–O isotope data from the Cook Austral Islands suggest that island mantle sources consist of recycled oceanic crust and mantle wedge material subducted with the slab (Lassiter et al., 2003). The HIMU isotopic compositions and low concentrations of fluid mobile elements are consistent with this source containing recycled and dehydrated oceanic crust. For the EMI source, the less radiogenic Os isotope compositions compared to HIMU preclude an origin from recycled sediments, and Lassiter et al. (2003) instead prefer an origin from subduction-modified mantle wedge material (Eiler et al., 1997). The similarity between our data and the Cook–Austral Islands implies these interpretations may well explain the same signatures in our samples.

The unradiogenic Hf isotope compositions in EMI samples compared to the mantle array is consistent with subduction-modified mantle wedge material as a source (Lassiter et al., 2003). Our data show the same unradiogenic Hf isotope signatures compared to the mantle array (see Supplementary Figure S4), reflecting decoupling of Lu/Hf and Sm/Nd in the EMI samples, in addition to the HIMU samples. Such decoupling may occur during partial melting with residual garnet. For example, radiogenic ingrowth in an E-MORB lava derived from melting peridotite containing residual garnet could possibly explain HIMU compositions (e.g. Ballentine et al., 1997; Blichert-Toft and Albarède, 1997; Davies et al., 2006). However, this alone cannot explain EMI compositions, which are less radiogenic than HIMU in Pb, Nd and Hf. EMI might be generated, though, through upper mantle metasomatism with melts generated with residual garnet (e.g. Eiler et al., 1997; Lassiter et al., 2003).

The isotopic evolution of metasomatized mantle material by such melts can be calculated in a very similar way to the model of Ballentine et al. (1997), who use a simple radiogenic ingrowth calculation to model HIMU Nd and Hf isotope compositions. We modified their three-stage model for Nd and Hf evolution by inserting parent/daughter ratios representing metasomatized upper mantle, modeled as DMM mixed with DMM melts that formed with residual garnet. We calculated the composition of a 10% batch melt of DMM (concentrations and D values from Salters and Stracke, 2004) and calculated parent daughter ratios for Nd, Hf and Pb isotopes for 5%, 10% and 25% melt addition (Supplementary Table S5). We then evaluated the effects if this event occurred at 3.5, 2.5, 1.5 and 0.5 Ga with the three-stage model. For Pb isotope evolution we modified the Stacey and Kramers (1975) model with a second-stage $\mu$ based on the calculated U/Pb elemental ratio starting at the time of metasomatism. This is a very rough estimate of the actual evolution in the Earth, but it demonstrates that DMM melting with residual garnet can decouple the Nd–Hf isotope systems and generate the unradiogenic Hf isotope signatures in ~1.5 Ga. Simultaneously, the partition coefficients for U and Pb are essentially identical between DMM and melt (Salters and Stracke, 2004), generating low $^{206}Pb/^{204}Pb$ compared to HIMU. The current parameters do not produce the lowest observed Nd isotope ratios and neither do changes in degree or type of melting or degree of metasomatism. However, slightly modified bulk Sm and Nd partition coefficients can achieve this (~0.075 and ~0.025, respectively). Therefore, our calculation shows that our data are consistent with the concept of recycled metasomatized mantle wedge, although the simplicity of the calculation relies on the interpretation of Os and O isotope data (e.g. Lassiter et al., 2003) to exclude a sedimentary origin for EMI.

In addition to the geochemical data and melting parameters being consistent with a metasomatic origin, the concept of recycling both the oceanic crust and metasomatized mantle is a logical combination in a subduction environment. The metasomatized material could be viscously coupled mantle wedge material, although it has also previously been suggested that MOR related upper mantle metasomatism can provide a source for OIVs after recycling the plate (e.g. Niu et al., 2002). Due to the lack of pristine trace element data in our current data set we cannot properly evaluate these two possibilities. However, either scenario provides a natural way to create HIMU and EMI sources in one subduction zone.

The generation of the observed isotope signatures requires residence in the mantle subsequent to subduction, but more importantly persistent eruption of isotopically distinct sources in three clusters requires a steady supply from these sources for over 100 Ma. Therefore, the Southwest Pacific mantle hosts several mantle source regions that have remained stable over this time. Moreover, the amount of melt erupted in the numerous seamounts related to the clusters of reconstructed eruptive locations requires involvement of even larger volumes of mantle sources, which are only partially molten. Since the upper mantle is generally considered to be convecting relatively rapidly, it cannot sustain large heterogeneities over several hundred Ma (van Keken et al., 2002). We therefore consider it more likely that these mantle sources are located in the lower mantle. We suggest that Cook–Austral mantle sources are anchored in a spatially fixed location (at least 100 Ma) in the lower mantle, and speculate that they have remained fixed in a dense layer of low-viscosity, previously subducted material (e.g. Jellinek and Manga, 2004). In this setting the Cook–Austral group of volcanoes most likely is the result of a group of plumes, each dominated by one distinct composition, and each active for a very long time (Schubert et al., 2004). Therefore, mantle plumes seem to provide the simplest model for the generation of these seamount chains, making it premature to retire the plume concept in favor of lithospheric extension.

## 6. Conclusions

The complicated age progression of the Cook–Austral Islands, Gilbert Ridge, Tokelau chain, and WPSP seamounts can be unraveled by tracing each volcano back to its eruptive location and fingerprinting them geochemically. The exceptionally long mantle geochemical records of these chains display three persistent clusters of mantle source regions, with distinct geochemical signatures, blurred by uncertainties in eruptive location reconstruction. The hotspot hypothesis, therefore, seems to explain these particular data rather well, while lithospheric extension is not required to explain the data, hence

Please cite this article as: Konter, J.G., et al., One hundred million years of mantle geochemical history suggest the retiring of mantle plumes is premature, Earth Planet. Sci. Lett. (2008), doi:10.1016/j.epsl.2008.08.023

rendering retirement of the hotspot hypothesis premature, even for a region with a rather complex history of intraplate volcanism.

## Acknowledgements

We thank the captain, crew, and shipmates on the RV Melville for helping with sample collection during the AVON02 expedition. We thank Kaj Hoernle, the Editor and an anonymous reviewer for valuable comments that significantly improved this manuscript. Initial ideas for color-coding compositions were developed at the 2004 CIDER workshop. This work was supported by the National Science Foundation (OCE 9102183, OCE 9730394, MRI-0079943, OCE-0453138, OCE-0241546, NSF-0549641) and the French Institut National des Sciences de l'Univers.

## Appendix A. Supplementary data

Supplementary data associated with this article can be found, in the online version, at doi:10.1016/j.epsl.2008.08.023.

## References

Altamimi, Z., Sillard, P., Boucher, C., 2002. ITRF2000; a new release of the international terrestrial reference frame for earth science applications. J. Geophys. Res. 107. doi:10.1029/2001JB000561.
Ballentine, C.J., Lee, D.-C., Halliday, A.N., 1997. Hafnium isotopic studies of the Cameroon line and new HIMU paradoxes. Chem. Geol. 139, 111–124.
Blichert-Toft, J., Albarède, F., 1997. The Lu–Hf isotope geochemistry of chondrites and the evolution of the mantle–crust system. Earth Planet. Sci. Lett. 148, 243–258.
Blichert-Toft, J., Chauvel, C., Albarède, F., 1997. Separation of Hf and Lu for high-precision isotope analysis of rock samples by magnetic sector-multi collector ICP-MS. Contrib. Mineral. Petrol. 127, 248–260.
Bonatti, E., Harrison, C.G.A., 1976. Hot lines in the Earth's mantle. Nature 263, 402–404.
Bryce, J.G., DePaolo, D.J., 2002. Pb isotopic heterogeneity in basaltic phenocrysts. Geochim. Cosmochim. Acta 68 (68), 4443–4468.
Chauvel, C., Blichert-Toft, J., 2001. A hafnium isotope and trace element perspective on melting of the depleted mantle. Earth Planet. Sci. Lett. 190, 137–151.
Chauvel, C., McDonough, W., Guille, G., Maury, R., Duncan, R., 1997. Contrasting old and young volcanism in Rurutu Island, Austral chain. Chem. Geol. 139, 125–143.
Courtillot, V., Davaille, A., Besse, J., Stock, J., 2003. Three distinct types of hotspots in the Earth's mantle. Earth Planet. Sci. Lett. 205, 295–308.
Davies, G.R., Stolz, A.J., Mahotkin, I.L., Nowell, G.M., Pearson, D.G., 2006. Trace element and Sr–Pb–Nd–Hf isotope Evidence for Ancient, fluid-dominated enrichment of the source of Aldan Shield lamproites. J. Petrol. 47, 1119–1146.
Davis, A.S., Pringle, M.S., Pickthorn, L.B.G., Clague, D.A., Schwab, W.C., 1989. Petrology and age of alkalic lava from the Ratak Chain of the Marshall Islands. J. Geophys. Res. 94, 5757–5774.
Dickinson, W.R., 1998. Geomorphology and geodynamics of the Cook–Austral Island–Seamount Chain in the South Pacific Ocean: implications for hotspots and plumes. Int. Geol. Rev. 40, 1039–1075.
Duncan, R.A., McCulloch, M.T., Barsczus, H.G., Nelson, D.R., 1986. Plume versus lithospheric sources for melts at Ua Pou, Marquesas Islands. Nature 322, 534–538.
Eiler, J.M., Farley, K.A., Valley, J.W., Hauri, E., Craig, H., Hart, S.R., Stolper, E.M., 1997. Oxygen isotope variations in ocean island basalt phenocrysts. Geochim. Cosmochim. Acta 61, 2281–2293.
Ekstrom, G., Dziewonski, A.M., 1998. The unique anisotropy of the Pacific upper mantle. Nature 394, 168–172.
Foulger, G.R., Natland, J.H., 2003. Is "hotspot" volcanism a consequence of plate tectonics? Science 300, 921–922.
Gans, K.D., Wilson, D.S., Macdonald, K.C., 2003. Pacific plate gravity lineaments: diffuse extension or thermal contraction. Geochem. Geophys. Geosyst. 4. doi:10.1029/2002GC000465.
Hanan, B.B., Graham, D.W., 1996. Lead and helium isotope evidence from oceanic basalts for a common deep source of mantle plumes. Science 272, 991–995.
Hanan, B.B., Blichert-Toft, J., Pyle, D., Christie, D., 2004. Contrasting origins of the upper mantle MORB source revealed by Hf and Pb isotopes from the Australian–Antarctic Discordance. Nature 432, 91–94.
Hanan, B.B., Shervais, J.W., Vetter, S.K., 2008. Yellowstone plume–continental lithosphere interaction beneath the Snake River Plain. Geology 36, 51–54.
Hart, S.R., 1984. A large-scale isotope anomaly in the Southern Hemisphere mantle. Nature 309, 753–757.
Hart, S.R., Hauri, E.H., Oschmann, L.A., Whitehead, J.A., 1992. Mantle plumes and entrainment — isotopic evidence. Science 256, 517–520.
Hauff, F., Hoernle, K., Schmidt, A., 2003. Sr–Nd–Pb composition of Mesozoic Pacific oceanic crust (site 1149 and 801, ODP Leg 185): implications for alteration of ocean crust and the input into the Izu–Bonin–Mariana subduction system. Geochem. Geophys. Geosyst. 4, 8913. doi:10.1029/2002GC000421.
Hoernle, K., Schmincke, H.-U., 1993. The petrology of the tholeiites through melilite nephelinites on Gran Canaria, Canary Islands: crystal fractionation, accumulation, and depths of melting. J. Petrol. 34, 573–597.
Hofmann, A.W., White, W.M., 1982. Mantle plumes from ancient oceanic-crust. Earth Planet. Sci. Lett. 57, 421–436.
Jackson, M.G., Hart, S.R., Koppers, A.A.P., Blusztajn, J., Staudigel, H., Konter, J., Kurz, M., Russell, J.A., 2007. Evidence for the return of subducted continental crust in Samoan lavas. Nature 448, 684–687.
Janney, P.E., Castillo, P.R., 1999. Isotope geochemistry of the Darwin Rise seamounts and the nature of long-term mantle dynamics beneath the south central Pacific. J. Geophys. Res. 104, 10571–10589.
Jellinek, A.M., Manga, M., 2004. Links between long-lived hotspots, mantle plumes, $D''$, and plate tectonics. Rev. Geophys. 42. doi:10.1029/2003RG000144.
Koppers, A.A.P., Staudigel, H., 2005. Asynchronous bends in Pacific seamount trails: a case for extensional volcanism? Science 307, 904–907.
Koppers, A.A.P., Morgan, J.P., Morgan, J.W., Staudigel, H., 2001. Testing the fixed hotspot hypothesis using Ar-40/Ar-39 age progressions along seamount trails. Earth Planet. Sci. Lett. 185, 237–252.
Koppers, A.A.P., Staudigel, H., Pringle, M.S., Wijbrans, J.R., 2003. Short-lived and discontinuous intraplate volcanism in the South Pacific: hotspots or extensional volcanism? Geochem. Geophys. Geosyst. 4. doi:10.1029/2003GC000533.
Koppers, A.A.P., Duncan, R.A., Steinberger, B., 2004. Implications of a nonlinear Ar-40/Ar-39 age progression along the Louisville seamount trail for models of fixed and moving hotspots. Geochem. Geophys. Geosyst. 5. doi:10.1029/2003GC000671.
Koppers, A.A.P., Staudigel, H., Phipps Morgan, J., Duncan, R.A., 2007. Nonlinear 40 Ar/39 Ar age systematics along the Gilbert Ridge and Tokelau Seamount Trail and the timing of the Hawaii–Emperor Bend. Geochem. Geophys. Geosyst. 8. doi:10.1029/2006GC001489.
Kroenke, L.W., Wessel, P., Sterling, A., 2004. Motion of the Ontong Java Plateau in the hot-spot frame of reference: 122 Ma–present. In: Fitton, J.G., Mahoney, J.J., Wallace, P.I., Saunders, A.D. (Eds.), Origin and Evolution of the Ontong Java Plateau. Geological Society, London, pp. 9–20.
Larson, R.L., 1991. Latest pulse of Earth: evidence for a mid-Cretaceous superplume. Geology 19, 963–966.
Lassiter, J.C., Blichert-Toft, J., Hauri, E.H., Barsczus, H.G., 2003. Isotope and trace element variations in lavas from Raivavae and Rapa, Cook–Austral islands: constraints on the nature of HIMU- and EM-mantle and the origin of mid-plate volcanism in French Polynesia. Chem. Geol. 202, 115–138.
Masters, G., Laske, G., Bolton, H., Dziewonski, A., 2000. The relative behavior of shear velocity, bulk sound speed, and compressional velocity in the mantle; implications for chemical and thermal structure. In: Karato, S., Forte, A.M., Liebermann, R.C., Masters, G., Stixrude, L. (Eds.), Geophysical Monograph. American Geophysical Union, Washington D.C., pp. 63–86.
McNutt, M.K., 1998. Superswells. Rev. Geophys. 36, 211–244.
McNutt, M.K., Fischer, K.M., 1987. The South Pacific superswell. Seamounts, Islands, and Atolls 43, 25–34.
McNutt, M.K., Caress, D.W., Reynolds, J., Jordahl, K.A., Duncan, R.A., 1997. Failure of plume theory to explain midplate volcanism in the Southern Austral Islands. Nature (London) 389, 479–482.
Menard, H.W., 1964. Marine geology of the Pacific. Marine geology of the Pacific 271.
Montagner, J.P., 2002. Upper mantle low anisotropy channels below the Pacific Plate. Earth Planet. Sci. Lett. 202, 263–274.
Montelli, R., Nolet, G., Dahlen, F.A., Masters, G., Engdahl, E.R., Hung, S.H., 2004. Finite-frequency tomography reveals a variety of plumes in the mantle. Science 303, 338–343.
Morgan, W.J., 1971. Convection plumes in the lower mantle. Nature 230, 42–43.
Niu, Y., Regelous, M., Wendt, I.J., Batiza, R., O'Hara, M., 2002. Geochemistry of near-EPR seamounts: importance of source vs. process and the origin of enriched mantle component. Earth Planet. Sci. Lett. 327–345.
O'Neill, C., Müller, D., Steinberger, B., 2005. On the uncertainties in hot spot reconstructions and the significance of moving hot spot reference frames. Geochem. Geophys. Geosyst. 6, Q04003. doi:10.1029/2004GC000784.
Raymond, C.A., Stock, J., Cande, S.C., 2000. Fast Paleogene motion of the Pacific hotspots from revised global plate circuit constraints. In: Richards, M.A., Gordon, R.G., Hilst, R.D.V.D. (Eds.), The History and Dynamics of Plate Motions. American Geophysical Union, Washington, DC, pp. 359–375.
Regelous, M., Hofmann, A.W., Abouchami, W., Galer, S.J.G., 2003. Geochemistry of lavas from the Emperor Seamounts, and the geochemical evolution of Hawaiian magmatism from 85 to 42 Ma. J. Petrol. 44, 113–140.
Romanowicz, B., Gung, Y.C., 2002. Superplumes from the core–mantle boundary to the lithosphere: implications for heat flux. Science 296, 513–516.
Salters, V.J.M., Stracke, A., 2004. Composition of the depleted mantle. Geochem. Geophys. Geosyst. 5. doi:10.1029/2003GC000597.
Sandwell, D., Fialko, Y., 2004. Warping and cracking of the Pacific plate by thermal contraction. J. Geophys. Res. 109. doi:10.1029/2004JB003091.
Shimizu, N., Hart, S.R., 1973. Differential dissolution technique (DDT): chemical separation of crystals from glass. Year Book Carnegie Inst. Washington 72, 268–270.
Schubert, G., Masters, G., Olson, P., Tackley, P., 2004. Superplumes or plume clusters? Phys. earth planet. inter. 146, 147–162.
Sleep, N.H., 1984. Tapping of magmas from ubiquitous mantle heterogeneities: an alternative to mantle plumes? J. Geophys. Res. 89, 10029–10042.
Smith, W.H.F., Staudigel, H., Watts, A.B., Pringle, M.S., 1989. The Magellan seamounts: early Cretaceous record of the South Pacific isotopic and thermal anomaly. J. Geophys. Res. 94, 10501–10523.
Stacey, J.S., Kramers, J.D., 1975. Approximation of terrestrial lead isotope evolution by a two-stage model. Earth Planet. Sci. Lett. 26, 207–221.
Staudigel, H., Park, K.H., Pringle, M., Rubenstone, J.L., Smith, W.H.F., Zindler, A., 1991. The longevity of the South-Pacific isotopic and thermal anomaly. Earth Planet. Sci. Lett. 102, 24–44.

Please cite this article as: Konter, J.G., et al., One hundred million years of mantle geochemical history suggest the retiring of mantle plumes is premature, Earth Planet. Sci. Lett. (2008), doi:10.1016/j.epsl.2008.08.023

Steinberger, B., 2000. Plumes in a convecting mantle: models and observations for individual hotspots. J. Geophys. Res.-Solid Earth 105, 11127–11152.
Steinberger, B., Sutherland, R., O'Connell, R.J., 2004. Prediction of Emperor–Hawaii seamount locations from a revised model of global plate motion and mantle flow. Nature 430, 167–173.
Tarduno, J.A., Duncan, R.A., Scholl, D.W., Cottrell, R.D., Steinberger, B., Thordarson, T., Kerr, B.C., Neal, C.R., Frey, F.A., Torii, M., Carvallo, C., 2003. The Emperor Seamounts: southward motion of the Hawaiian hotspot plume in earth's mantle. Science 301, 1064–1069.
Todt, W., Cliff, R., Hanser, A., Hofmann, A.W., 1996. Evaluation of a $^{202}$Pb–$^{205}$Pb double spike for high precision lead isotope analysis. In: Hart, S.R., Basu, A. (Eds.), Earth Processes: Reading the Isotopic Code. AGU, pp. 429–437.
van Keken, P.E., Hauri, E.H., Ballentine, C.J., 2002. Mantle mixing: the generation, preservation, and destruction of chemical heterogeneity. Ann. Rev. Earth Planet. Sci. 30, 493–525.
Weiss, D., Kieffer, B., Maerschalk, C., Barling, J., de Jong, J., Williams, G.A., Hanano, D., Pretorius, W., Mattieli, N., Scoates, J.S., Goolaerts, A., Friedman, R.M., Mahoney, J.B., 2006. High-precision isotopic characterization of USGS reference materials by TIMS and MC-ICP-MS. Geochem. Geophys. Geosyst. 7. doi:10.1029/2006GC001283.
Wessel, P., Kroenke, L., 1997. A geometric technique for relocating hotspots and refining absolute plate motions. Nature 387, 365–369.
Wessel, P., Kroenke, L.W., 2008. Pacific absolute plate motion since 145 Ma: an assessment of the fixed hot spot hypothesis. J. Geophys. Res. 113. doi:10.1029/2007JB005499.
Wessel, P., Harada, Y., Kroenke, L.W., 2006. Toward a self-consistent, high-resolution absolute plate motion model for the Pacific. Geochem. Geophys. Geosyst. 7. doi:10.1029/2005GC001000.
White, W.M., Hofmann, A.W., 1982. Sr and Nd isotope geochemistry of oceanic basalts and mantle evolution. Nature 296, 821–825.
White, W.M., Patchett, J., 1984. Hf–Nd–Sr isotopes and incompatible element abundances in island arcs — implications for magma origins and crust–mantle evolution. Earth Planet. Sci. Lett. 67, 167–185.
White, W.M., Albarede, F., Telouk, P., 2000. High-precision analysis of Pb isotope ratios by multi-collector ICP-MS. Chem. Geol. 167, 257–270.
Willbold, M., Stracke, A., 2006. Trace element composition of mantle end-members: implications for recycling of oceanic and upper and lower continental crust. Geochem. Geophys. Geosyst. 7. doi:10.1029/2005GC001005.
Winterer, E.L., Natland, J.H., van Waasbergen, R.J., Duncan, R.A., McNutt, M.K., Wolfe, C.J., Silva, I.P., Sager, W.W., Sliter, W.V., 1993. Cretaceous guyots in the northwest Pacific: an overview of their geology and geophysics. The Mesozoic Pacific: Geology, Tectonics, and Volcanism 77, 307334.
Wolfe, C.J., McNutt, M.K., 1991. Compensation of cretaceous seamounts of the Darwin Rise, northwest Pacific Ocean. J. Geophys. Res. 96, 2363–2374.
Woodhead, J.D., 1992. Temporal geochemical evolution in oceanic intra-plate volcanics: a case study from the Marquesas (French Polynesia) and comparison with other hotspots. Contrib. Mineral. Petrol. 111, 458–467.
Workman, R.K., Hart, S.R., 2005. Major and trace element composition of the depleted MORB mantle(DMM). Earth Planet. Sci. Lett. 231, 53–72.
Workman, R., Hart, S.R., Jackson, M., Regelous, M., Farley, K.A., Blusztajn, J., Kurz, M., Staudigel, H., 2004. Recycled metasomatized lithosphere as the origin of the Enriched Mantle II (EM2) end-member: evidence from the Samoan Volcanic Chain. Geochem. Geophys. Geosyst. 5. doi:10.1029/2003GC000623.
Zindler, A., Hart, S., 1986. Chemical geodynamics. Ann. Rev. Earth Planet. Sci. 14, 493–571.

Please cite this article as: Konter, J.G., et al., One hundred million years of mantle geochemical history suggest the retiring of mantle plumes is premature, Earth Planet. Sci. Lett. (2008), doi:10.1016/j.epsl.2008.08.023